Synaptic Inputs to Displaced Intrinsically-Photosensitive Ganglion Cells in Macaque Retina

Andrea Bordt
McGovern Medical School
Sara S. Patterson
University of Rochester
James A. Kuchenbecker
University of Washington
Marcus A. Mazzaferri
University of Washington
Joel N. Yearick
Rice University
Emma R. Yang
Rice University
Judith Mosinger Ogilvie
Saint Louis University
Jay Neitz
University of Washington
David W. Marshak (david.w.marshak@uth.tmc.edu)
McGovern Medical School

Research Article

Keywords: vision, bipolar cells, amacrine cells, primate, electron microscopy, connectomics
RRID:SCR_003584, RRID:SCR_005986, RRID: SCR_001622, RRID: SCR_017350

Posted Date: February 15th, 2022

DOI: https://doi.org/10.21203/rs.3.rs-1239828/v1

Abstract

Ganglion cells are the projection neurons of the retina. Intrinsically photosensitive retinal ganglion cells (ipRGCs) express the photopigment melanopsin and also receive input from rods and cones via bipolar cells and amacrine cells. In primates, multiple types of ipRGCs have been identified. The ipRGCs with somas in the ganglion cell layer have been studied extensively, but less is known about those with somas in the inner nuclear layer, the “displaced” cells. To investigate their synaptic inputs, three sets of horizontal, ultrathin sections through central macaque retina were collected using serial blockface scanning electron microscopy. One displaced ganglion cell with a smaller soma and lipofuscin granules was classified as a displaced M1 cell. It received nearly all of its excitatory inputs from ON bipolar cells and would have ON responses to light. In all three volumes, there were cells in the inner nuclear layer that had extremely large somas, varicose axons and dendrites with a large diameter that formed a sparse arbor in the outermost stratum of the inner plexiform layer. They were identified as the gigantic displaced M1 type of ipRGCs based on this morphology and on the high density of granules in their somas. They received extensive input from amacrine cells. The vast majority of their excitatory inputs were from OFF bipolar cells, and they would have OFF responses to light stimuli under some conditions, like the novel type of ipRGCs described recently in humans. They may account for the paradoxical pupillary responses seen in some patients with congenital stationary night blindness.

Introduction

In primates, there are multiple types of retinal ganglion cells that differ in their morphology, synaptic inputs, light responses and central projections [1]. These include intrinsically photosensitive retinal ganglion cells (ipRGCs), which express the photopigment melanopsin and respond to light directly. They also receive input from rods and cones via excitatory synapses from bipolar cells and inhibitory synapses from amacrine cells. Their central projections include the suprachiasmatic nucleus of the hypothalamus, the dorsal lateral geniculate nucleus and the pretectal olivary nucleus [2].

Mice have at least six types of ipRGCs with distinct morphology, light responses and central projections [3]. However, it is uncertain how many types of ipRGCs exist in primates. Initially, the primate ipRGCs were divided into two types: outer-stratifying cells, also known as M1, whose dendrites branched in the first stratum (S1) of the inner plexiform layer (IPL), and inner-stratifying cells, also known as M2, whose dendrites branched in the fifth stratum (S5)[4]. More recent studies indicate that there is greater diversity of primate ipRGCs. Using light microscopic immunolabeling in human retina, six types were identified using soma size and position, dendritic arbor size and stratification and the levels of melanopsin expression[5]. Based on patterns of gene expression, three types were identified in peripheral macaque retina[6]. Three types of extracellularly recorded light responses have been observed in human ipRGCs[7].

We have adopted a different approach to study the diversity of ipRGCs in primates. We reconstructed retinal ganglion cells from images obtained by serial block-face scanning electron microscopy (SBFSEM) of central macaque retina. We identified ipRGCs by their sparse dendritic arbors, their narrow stratification

in the IPL and their axonal morphology and then reconstructed the presynaptic neurons. In one volume located approximately 1.5 mm inferior to the center of the fovea, we identified two types of ipRGCs with somas in the ganglion cell layer (GCL). The first received extensive inhibitory input from short wavelength-sensitive (S) cones via S-ON bipolar cells and S-cone amacrine cells, as well as excitatory input from both ON and OFF bipolar cells. It resembled the M1 morphological type, and its dendrites ramified mainly in S1 of the IPL[8]. A second type resembled the M2 ipRGCs morphologically, with sparse dendrites ramifying entirely in S5 of the IPL. They received direct, excitatory input from ON bipolar cells, almost exclusively from the S-ON type[9].

Here we report the synaptic inputs to ipRGCs with somas located in the inner nuclear layer (INL), which are also known as displaced ganglion cells. In each of three volumes taken from different quadrants of the central retina, we found large ipRGCs that ramified narrowly in S1 of the IPL and received excitatory input almost entirely from OFF bipolar cells. These resembled the gigantic displaced M1 cells[5], and they may account for the OFF responses to light reported in human ipRGCs[7]. In the volume inferior to the fovea, we identified another displaced ipRGC with a smaller soma and some dendrites that descended into the innermost stratum of the IPL. This smaller ipRGC received excitatory inputs almost exclusively from ON bipolar cells, as expected from previous light microscopic studies of displaced ipRGCs in primates[4].

Methods

All methods were performed in accordance with the relevant guidelines and regulations.

Electron Microscopy

Retinal tissue was obtained from a terminally anesthetized, adult male macaque (*Macaca nemestrina*) through the Tissue Distribution Program at the Washington National Primate Center. All procedures were approved by the Institutional Animal Care and Use Committee at the University of Washington. Central retinal tissue was processed for SBFSEM as previously described[10]. Briefly, three 1 x 1 mm square blocks were fixed in glutaraldehyde, stained *en bloc* with osmium ferrocyanide, uranyl acetate and lead aspartate and then embedded in epoxy resin. The selected areas, ranging from 1.25 to 2 mm from the center of the fovea, were particularly well-suited for connectomic analysis because most of the neurons were small, and the high spatial density of retinal ganglion cells facilitated the identification of rare types. The images were acquired using a Zeiss Sigma VP field emission scanning electron microscope equipped with a 3View system (Gatan, Inc.). See Table 1 for details.

Table 1

Quadrant	Eccentricity	Section Thickness	Number of Sections	Dimensions	Resolution
Temporal	~ 2 mm	70 nm	937	220 x 200 μm	7.5 nm/pixel
Inferior	~1.5 mm	95 nm	1835	240 x 230 μm	7.5 nm/pixel
Nasal	~1.25 mm	50 nm	2354	170 x 180 μm	5 nm/pixel

Connectomic analysis

Three retinal volumes, sectioned in the horizontal plane and acquired at resolutions of 5 nm/pixel or 7.5 nm/pixel, were studied. Two of these volumes were also used in recent studies of synaptic inputs to other types of retinal ganglion cells[8–12]. Image registration was performed using Nornir (http://nornir.github.io RRID:SCR_003584), and the image tiles were reassembled into cohesive digital volumes and hosted on a 24-core server at the University of Washington.

The serial EM volumes were annotated using the web-based, multiuser Viking software described previously[13] (RRID:SCR_005986). Briefly, profiles of processes were typically annotated by placing circular discs with the same diameter at their centers of mass and linking them to annotations on adjacent sections. In some instances, neurons were annotated with closed curves in order to provide more realistic reconstructions. Synaptic densities were annotated with lines and linked to the neurons in which they were located. Neurons and other structures were numbered consecutively. The boundary between the INL and the inner plexiform layer (IPL) was designated as 0% and the IPL-GCL boundary as 100% depth. The IPL was divided into 5 strata of 20% each, with 1 beginning at the INL and 5 ending at the GCL.

The major cell types were identified using ultrastructural criteria[14–16]. Axon terminals of bipolar cells contained numerous synaptic vesicles and synaptic ribbons. We confirmed the identity of the presynaptic bipolar cells by reconstructing the axon terminals and, wherever possible, the somas and primary dendrites. Axons and dendrites of amacrine cells contained fewer synaptic vesicles, and they were typically clustered at synapses. In all, four ipRGCs and the neurons providing their inputs were annotated. The data are available to the public on a read-only basis (http://connectomes.utah.edu). The volume addresses are:

inferior: http://v2486.host.s.uw.edu/Neitz/InferiorMonkey/SliceToVolume.vikingxml

temporal: http://v2486.host.s.uw.edu/Neitz/TemporalMonkey2/SliceToVolume.vikingxml

nasal: http://v2486.host.s.uw.edu/Neitz/NM/SliceToVolume.vikingxml.

Data Analysis

Data analysis and three dimensional rendering were performed using an open-source Matlab (Mathworks, RRID: SCR_001622) program https://github.com/neitzlab/sbfsem-tools RRID: SCR_017350 and Tulip (https://tulip.labri.fr/site/). The image rendering was performed using the RenderApp function[17]. Using the SynapseSphere function, synapses were rendered as unit spheres centered at each synapse annotation's X, Y and Z coordinates then scaled to optimize visibility. Processes of ipRGCs and axon terminals of bipolar cells were analyzed using the IPLDepth function[12]. The dendrites of ipRGCs were analyzed using the singleDendriteDiameter function[11], and the soma diameters were determined using the Measure Line (Mosaic) tool in Viking.

Figures

Figures were prepared using Adobe Photoshop CS6 and SBFSEM-tools. Whenever possible, the color palette was selected so that the figures could be interpreted by individuals with all of the common forms of color blindness using Photoshop and the websites https://davidmathlogic.com/colorblind/ and http://mkweb.bcgsc.ca/colorblind/. The code and data used to generate the figures in this study will be made available upon request.

Results

Displaced ipRGCs

The somas of ipRGCs in the INL were clearly distinguishable from those of other types of cells (Figure 1). The somas were considerably larger than those of the surrounding amacrine or bipolar cells, and they contained numerous lipofuscin granules. They had varicose axons that arose from the soma or from a primary dendrite (Figure 2). The dendrites also had a large diameter, and they branched infrequently. The dendritic arbors were large, but it was not possible to determine their exact size because they exceeded the dimensions of the volumes that were analyzed. The nasal and temporal volumes each contained one displaced ipRGC with a large soma and dendrites confined to S1 of the IPL. These cells, 6210 temporal and 11354 nasal, were classified as the gigantic displaced M1 type[18].

In the inferior volume, there were two distinct types of displaced ipRGCs, and because they were located nearby, they could be compared directly (Figure 2). Cell 1178 was classified as the gigantic M1 type on the basis of its size and dendritic stratification. The soma was ovoid and its maximum diameter, measured before the primary dendrites had emerged, was 16.6 by 23.7 μm. The mean diameter of the primary dendrite was 2.8 ± 1.12 (s.d.) μm. The diameters of the secondary dendrites were 2.06 ± 0.44 μm, and 1.27 ± 0.43 μm. The diameters of the tertiary dendrites were 1.36 ± 0.48 μm and 1.24 ± 0.38. Cell 21551 had a smaller soma with a maximum diameter of 14.7 by 14.4 μm. Its primary dendrite was short and had a mean diameter of 1.13 ± 0.11 μm. The diameters of its secondary dendrites were: 0.90 ± 0.83 μm, 1.17 ± 0.37 μm, 1.04 ± 0.35 μm and 1.54 ± 0.30 μm. Its proximal dendrites ramified in S1, and in this respect, it resembled the displaced M1 type[18]. However, the distal dendrites of cell 21551 ramified in S4 and S5.

Presynaptic amacrine cells

All four displaced ipRGCs received the majority of their synaptic inputs from unidentified amacrine cells (Figures 1 & 3). The proportion of input from amacrine cells varied in the three quadrants. Amacrine cells were presynaptic at 76% (180/236) of synapses in the nasal volume, 85% in the inferior volume (167/197) and 88% in the temporal volume (255/289). Based on previous immunolabeling studies, inputs from dopaminergic amacrine cells were expected[5,19]. An amacrine cell with the large somas and dendrites ramifying in S1 characteristic of dopaminergic amacrine cells was partially reconstructed in the nasal volume (not illustrated), but no synapses from its dendrites onto the gigantic displaced M1 ipRGC were found. One amacrine cell axon that made 12 synapses onto the soma and primary dendrites of ipRGC 1178 in the inferior volume was partially reconstructed (Figure 4). Based on its pattern of synaptic connections and its narrowly stratified arbor in S1 and the INL, it likely originated from a dopaminergic amacrine cell. Taken together, these findings suggest that dopaminergic inputs to ipRGCs are mediated by the axons originating from somas outside the volume.

Presynaptic bipolar cells

Ribbons surrounded by a halo of vesicles were found at most of the synapses from bipolar cells onto ipRGCs, but they were absent at some of the synapses. This is not attributable to the low contrast of synaptic ribbons in this material. In each instance, the bipolar cells were annotated sufficiently to verify that ribbons were present at other synapses, and many of the presynaptic bipolar cells were identified morphologically. The best-characterized example was found in the nasal volume (Figure 5). Synaptic densities and vesicles were observed in 18 consecutive 50 nm sections, but there was no associated ribbon. Synaptic ribbons were found elsewhere in the axon terminal of this bipolar cell. In the nasal volume, 71% (40/56) of the bipolar cell synapses onto ipRGC 11354 had synaptic ribbons associated with the synaptic density, but the remainder did not.

The vast majority of the excitatory inputs to the gigantic displaced M1 cells were from OFF bipolar cells. Excitatory inputs to the cell that was reconstructed most completely, 11345 in the nasal volume, came from one presynaptic ON bipolar cell and 27 OFF bipolar cells. The results with the other two displaced gigantic M1 cells were very similar. The presynaptic bipolar cells were partially reconstructed and classified based on their morphology [16,20]. Three distinct types of bipolar cells were presynaptic to the gigantic displaced M1 ipRGCs (Figures 6 & 7). Diffuse bipolar 1 (DB1) cells had delicate axon terminals that formed arbors with relatively large diameters that were restricted to S1 of the IPL. DB2 bipolar cells had more rugose axon terminals that formed arbors with somewhat smaller diameters that occupied part of S1 as well as S2 of the IPL. The axon terminals of OFF midget bipolar cells were found in the same strata as those of DB2, but they could be distinguished by the very small diameters of their axonal arbors. Some of the presynaptic bipolar cells could not be identified, but they could be reconstructed sufficiently to determine that they ramified in either S1, S2 or both strata of the IPL.

At least four types of bipolar cells were presynaptic to the displaced M1 ipRGC in the inferior connectome, cell 21551 (Figure 8). One presynaptic bipolar cell was identified as DB1 using the criteria described above, and it made the only synapse from an OFF bipolar cell. The rest of the synapses originated from ON bipolar cells. Two were identified as the S-ON type based on their contacts with small bistratified ganglion cells and S-cone amacrine cells[8,10]. Two other presynaptic bipolar cells that had axonal arbors in S5 with a larger diameter were identified as the DB6 type. One other presynaptic bipolar cell with a large dendritic arbor centered around the border between S4 and S5 was clearly diffuse. It was positively identified as DB5 by reconstructing a population of neighboring DB4 and DB5 bipolar cell axon terminals. Its axon terminal filled a gap in the mosaic of DB5 terminals, but it overlapped with the terminals of a DB4 cell. Four presynaptic bipolar cells with relatively small axon terminals that ramified around the same level in the IPL were classified as ON midget cells[16,20]. One synapse onto the displaced M1 ipRGC was made by a bipolar cell with a very narrow axonal arbor ramifying between 70% and 90% depth in the IPL. It closely resembled the rod bipolar cells identified at the same eccentricity in an electron microscopic immunolabeling study of macaque retina [21].

Discussion

The gigantic displaced M1 ganglion cells of human retina are a distinct type based on their morphology[5,22], and the data reported here on the preponderance of excitatory synaptic inputs from OFF bipolar cells to their homologs in macaque retina support this finding. This is the first study to identify the types of bipolar cells that provide input to displaced ipRGCs using electron microscopy (EM). Some of these synapses from bipolar cells were not associated with synaptic ribbons. In this respect, they were similar to synapses described previously using EM. In salamander and rabbit retinas, synapses like these were seen using serial, ultrathin sections [23–25]. These synapses may also account for the images of excitatory synapses without synaptic ribbons observed in macaque retinas using freeze-fracture [26].

The gigantic displaced M1 cells would be expected to generate rapid, transient excitatory responses to decrements in light intensity and, initially, very little response to light increments. If the stimulus intensity exceeded the threshold to activate melanopsin, a sustained, excitatory response would be expected to follow after a delay. Additional experiments using intracellular recordings with tracer injections in macaque retina would be required to confirm the identity of the cells. However, all the published recordings using these techniques in primate retinas have been from ipRGCs with somas in the GCL [27]. Transient OFF responses mediated by inputs from bipolar cells have been described in a subset of human ipRGCs recorded extracellularly with multi-electrode arrays [7]. Because M1 cells with somas in the GCL also receive some excitatory inputs from OFF bipolar cells [8], it is uncertain whether those responses were generated by neurons with somas in the GCL or in the INL. If they project to the same targets in the brain, the OFF responses from ipRGCs would be expected to oppose the actions of ON responses of the other ipRGCs, increasing the operating range of the rapid component of the non-image forming visual system.

The excitatory inputs to gigantic displaced M1 ipRGCs came from three different types of OFF bipolar cells: DB1, DB2 and OFF midget. These would be expected to respond to decreases in light intensity under a wide range of ambient light intensities. In scotopic conditions, they would receive signals from the primary rod pathway via AII amacrine cells, which provide extensive input to DB1 and OFF midget bipolar cells. Under photopic conditions, those bipolar cells would receive crossover inhibition from the AII cells and convey this to the ganglion cells [28]. Both DB1 and OFF midget bipolar cells have sustained responses to light mediated by their voltage-gated conductances and the kainate receptors on their dendrites. The voltage-gated conductances and kainate receptors of DB2 cells generate rapid, transient responses [28–30]. Together, the three types of OFF bipolar cells would generate robust responses to decrements in light intensity in displaced gigantic M1 ipRGCs.

The displaced M1 ganglion cell 21551 in the inferior volume received the majority of its excitatory input from multiple types of ON-type cone bipolar cells, including: S-ON, ON midget, DB5 and DB6 bipolar cells. These inputs would be expected to generate light responses in the displaced M1 ganglion cell under a wide variety of conditions. The ON midget bipolar cells receive input from the primary rod pathway via AII amacrine cells [31]. The DB5 bipolar cells have T-type voltage-gated calcium currents and are expected to have transient responses to light onset. Based on their voltage-gated currents, DB6 and ON midget ganglion cells are expected to have more sustained responses to light onset [29]. S-ON bipolar cells have not been studied directly, but, based on their expression of metabotropic glutamate receptors and the responses of their postsynaptic cells, they are expected to have sustained ON responses to short wavelength lights in their receptive field centers[32,33]

A previous light microscopic study found that DB6 bipolar cells contacted ipRGCs [4,34] and we confirmed that these contacts are synapses. One of the excitatory synapses onto displaced M1 ganglion cell 21551 was made by a rod bipolar cell. The same was true of an M1 ipRGC with its soma in the GCL[8]. This finding had also been predicted using light microscopic immunolabeling in human retinas[5]. However, in other studies of macaque retinas, no contacts between immunolabeled ipRGCs and rod bipolar cells were observed, and rod bipolar cells did not make synapses onto ganglion cell dendrites [21,34]. This discrepancy may be attributable to undersampling. The spatial density of displaced M1 ipRGC somas is very low, their dendritic arbors are sparse, and only one of the excitatory inputs in our study was from an identified rod bipolar cell. Synapses like these would be very rarely encountered. For example, in a study of seven fully-reconstructed rod bipolar cells in the rabbit retina, only two synapses onto retinal ganglion cells were reported [24].

The visual input for the pupillary reflex is mediated by projections of ipRGCs to the olivary pretectal nucleus [35,36]. Input from the gigantic displaced M1 cells and other ipRGCs with OFF bipolar cell input might account for paradoxical pupil response seen in some patients with congenital stationary night blindness, whose ON pathway is not functional [37,38]. When the ambient light is turned off, their pupils constrict transiently instead of dilating as expected. This could be explained if input from ipRGCs with OFF responses is normally opposed by stronger input from ipRGCs with ON responses. In these patients,

the OFF input would initially control the pupil diameter until the excitatory input mediated by melanopsin prevails.

Declarations

Acknowledgments:

This research was supported by NIH grants EY027859, EY002576, NS099578, EY007031, EY007125, EY032318, P51-OD010425/ORID and P30-EY001730 and Research to Prevent Blindness. Implementation of the Viking software environment for image capture, registration, database, and annotation was supported through NIH grants to Bryan William Jones (R01-EY015128, R01-EY028927)

References

1 Grünert, U. & Martin, P. R. Morphology, Molecular Characterization, and Connections of Ganglion Cells in Primate Retina. *Annual review of vision science***7**, 73-103, doi:10.1146/annurev-vision-100419-115801 (2021).

2 Do, M. T. H. Melanopsin and the Intrinsically Photosensitive Retinal Ganglion Cells: Biophysics to Behavior. *Neuron***104**, 205-226, doi:10.1016/j.neuron.2019.07.016 (2019).

3 Vidal-Villegas, B. *et al.* Photosensitive ganglion cells: A diminutive, yet essential population. *Archivos de la Sociedad Espanola de Oftalmologia***96**, 299-315, doi:10.1016/j.oftale.2020.06.020 (2021).

4 Liao, H. W. *et al.* Melanopsin-expressing ganglion cells on macaque and human retinas form two morphologically distinct populations. *The Journal of comparative neurology***524**, 2845-2872, doi:10.1002/cne.23995 (2016).

5 Hannibal, J., Christiansen, A. T., Heegaard, S., Fahrenkrug, J. & Kiilgaard, J. F. Melanopsin expressing human retinal ganglion cells: Subtypes, distribution, and intraretinal connectivity. *The Journal of comparative neurology***525**, 1934-1961, doi:10.1002/cne.24181 (2017).

6 Peng, Y. R. *et al.* Molecular Classification and Comparative Taxonomics of Foveal and Peripheral Cells in Primate Retina. *Cell***176**, 1222-1237 e1222, doi:10.1016/j.cell.2019.01.004 (2019).

7 Mure, L. S., Vinberg, F., Hanneken, A. & Panda, S. Functional diversity of human intrinsically photosensitive retinal ganglion cells. *Science (New York, N.Y.)***366**, 1251-1255, doi:10.1126/science.aaz0898 (2019).

8 Patterson, S. S., Kuchenbecker, J. A., Anderson, J. R., Neitz, M. & Neitz, J. A Color Vision Circuit for Non-Image-Forming Vision in the Primate Retina. *Current biology : CB***30**, 1269-1274 e1262, doi:10.1016/j.cub.2020.01.040 (2020).

9 Patterson, S. S. *et al.* Another Blue-ON ganglion cell in the primate retina. *Current biology : CB***30**, R1409-R1410, doi:10.1016/j.cub.2020.10.010 (2020).

10 Patterson, S. S. *et al.* An S-cone circuit for edge detection in the primate retina. *Scientific reports***9**, 11913, doi:10.1038/s41598-019-48042-2 (2019).

11 Bordt, A. S. *et al.* Synaptic inputs to broad thorny ganglion cells in macaque retina. *The Journal of comparative neurology***529**, 3098-3111, doi:10.1002/cne.25156 (2021).

12 Patterson, S. S. *et al.* Wide-field amacrine cell inputs to ON parasol ganglion cells in macaque retina. *The Journal of comparative neurology***528**, 1588-1598, doi:10.1002/cne.24840 (2020).

13 Anderson, J. R. *et al.* The Viking viewer for connectomics: scalable multi-user annotation and summarization of large volume data sets. *Journal of microscopy***241**, 13-28, doi:10.1111/j.1365-2818.2010.03402.x (2011).

14 Dowling, J. E. & Boycott, B. B. Organization of the primate retina: electron microscopy. *Proceedings of the Royal Society of London. Series B, Biological sciences***166**, 80-111 (1966).

15 Tsukamoto, Y. & Omi, N. OFF bipolar cells in macaque retina: type-specific connectivity in the outer and inner synaptic layers. *Frontiers in neuroanatomy***9**, 122, doi:10.3389/fnana.2015.00122 (2015).

16 Tsukamoto, Y. & Omi, N. ON Bipolar Cells in Macaque Retina: Type-Specific Synaptic Connectivity with Special Reference to OFF Counterparts. *Frontiers in neuroanatomy***10**, 104, doi:10.3389/fnana.2016.00104 (2016).

17 Bordt, A. S. *et al.* Synaptic inputs from identified bipolar and amacrine cells to a sparsely branched ganglion cell in rabbit retina. *Visual neuroscience***36**, E004, doi:10.1017/s0952523819000014 (2019).

18 Hannibal, J. *et al.* Gene expression of pituitary adenylate cyclase activating polypeptide (PACAP) in the rat hypothalamus. *Regul Pept***55**, 133-148 (1995).

19 Hattar, S., Liao, H. W., Takao, M., Berson, D. M. & Yau, K. W. Melanopsin-containing retinal ganglion cells: architecture, projections, and intrinsic photosensitivity. *Science (New York, N.Y.)***295**, 1065-1070, doi:10.1126/science.1069609 (2002).

20 Boycott, B. B. & Wassle, H. Morphological Classification of Bipolar Cells of the Primate Retina. *Eur J Neurosci***3**, 1069-1088 (1991).

21 Grunert, U. & Martin, P. R. Rod bipolar cells in the macaque monkey retina: immunoreactivity and connectivity. *The Journal of neuroscience : the official journal of the Society for Neuroscience***11**, 2742-2758 (1991).

22 Chandra, A. J., Lee, S. C. S. & Grünert, U. Melanopsin and calbindin immunoreactivity in the inner retina of humans and marmosets. *Visual neuroscience* **36**, E009, doi:10.1017/s0952523819000087 (2019).

23 Lauritzen, J. S. *et al.* ON cone bipolar cell axonal synapses in the OFF inner plexiform layer of the rabbit retina. *The Journal of comparative neurology* **521**, 977-1000, doi:10.1002/cne.23244 (2013).

24 Strettoi, E., Dacheux, R. F. & Raviola, E. Synaptic connections of rod bipolar cells in the inner plexiform layer of the rabbit retina. *The Journal of comparative neurology* **295**, 449-466, doi:10.1002/cne.902950309 (1990).

25 Wong-Riley, M. T. Synaptic orgnization of the inner plexiform layer in the retina of the tiger salamander. *Journal of neurocytology* **3**, 1-33 (1974).

26 Raviola, E. & Raviola, G. Structure of the synaptic membranes in the inner plexiform layer of the retina: a freeze-fracture study in monkeys and rabbits. *The Journal of comparative neurology* **209**, 233-248, doi:10.1002/cne.902090303 (1982).

27 Dacey, D. M. *et al.* Melanopsin-expressing ganglion cells in primate retina signal colour and irradiance and project to the LGN. *Nature* **433**, 749-754, doi:10.1038/nature03387 (2005).

28 McLaughlin, A. J., Percival, K. A., Gayet-Primo, J. & Puthussery, T. Glycinergic Inhibition Targets Specific Off Cone Bipolar Cells in Primate Retina. *eNeuro* **8**, doi:10.1523/eneuro.0432-20.2020 (2021).

29 Puthussery, T., Venkataramani, S., Gayet-Primo, J., Smith, R. G. & Taylor, W. R. NaV1.1 channels in axon initial segments of bipolar cells augment input to magnocellular visual pathways in the primate retina. *The Journal of neuroscience : the official journal of the Society for Neuroscience* **33**, 16045-16059, doi:10.1523/jneurosci.1249-13.2013 (2013).

30 Puthussery, T. *et al.* Kainate receptors mediate synaptic input to transient and sustained OFF visual pathways in primate retina. *The Journal of neuroscience : the official journal of the Society for Neuroscience* **34**, 7611-7621, doi:10.1523/jneurosci.4855-13.2014 (2014).

31 Haverkamp, S., Haeseleer, F. & Hendrickson, A. A comparison of immunocytochemical markers to identify bipolar cell types in human and monkey retina. *Visual neuroscience* **20**, 589-600 (2003).

32 Crook, J. D. *et al.* Parallel ON and OFF cone bipolar inputs establish spatially coextensive receptive field structure of blue-yellow ganglion cells in primate retina. *The Journal of neuroscience : the official journal of the Society for Neuroscience* **29**, 8372-8387, doi:10.1523/jneurosci.1218-09.2009 (2009).

33 Dacey, D. M. & Lee, B. B. The 'blue-on' opponent pathway in primate retina originates from a distinct bistratified ganglion cell type. *Nature* **367**, 731-735, doi:10.1038/367731a0 (1994).

34 Grunert, U., Jusuf, P. R., Lee, S. C. & Nguyen, D. T. Bipolar input to melanopsin containing ganglion cells in primate retina. *Visual neuroscience* **28**, 39-50, doi:10.1017/s095252381000026x (2011).

35 Gamlin, P. D. The pretectum: connections and oculomotor-related roles. *Progress in brain research***151**, 379-405, doi:10.1016/s0079-6123(05)51012-4 (2006).

36 Hannibal, J. *et al.* Central projections of intrinsically photosensitive retinal ganglion cells in the macaque monkey. *The Journal of comparative neurology***522**, 2231-2248, doi:10.1002/cne.23588 (2014).

37 Myers, G. A., Barricks, M. E. & Stark, L. Paradoxic pupillary constriction in a patient with congenital stationary night blindness. *Investigative ophthalmology & visual science***26**, 736-740 (1985).

38 Price, M. J., Thompson, H. S., Judisch, G. F. & Corbett, J. J. Pupillary constriction to darkness. *The British journal of ophthalmology***69**, 205-211, doi:10.1136/bjo.69.3.205 (1985).

Figures

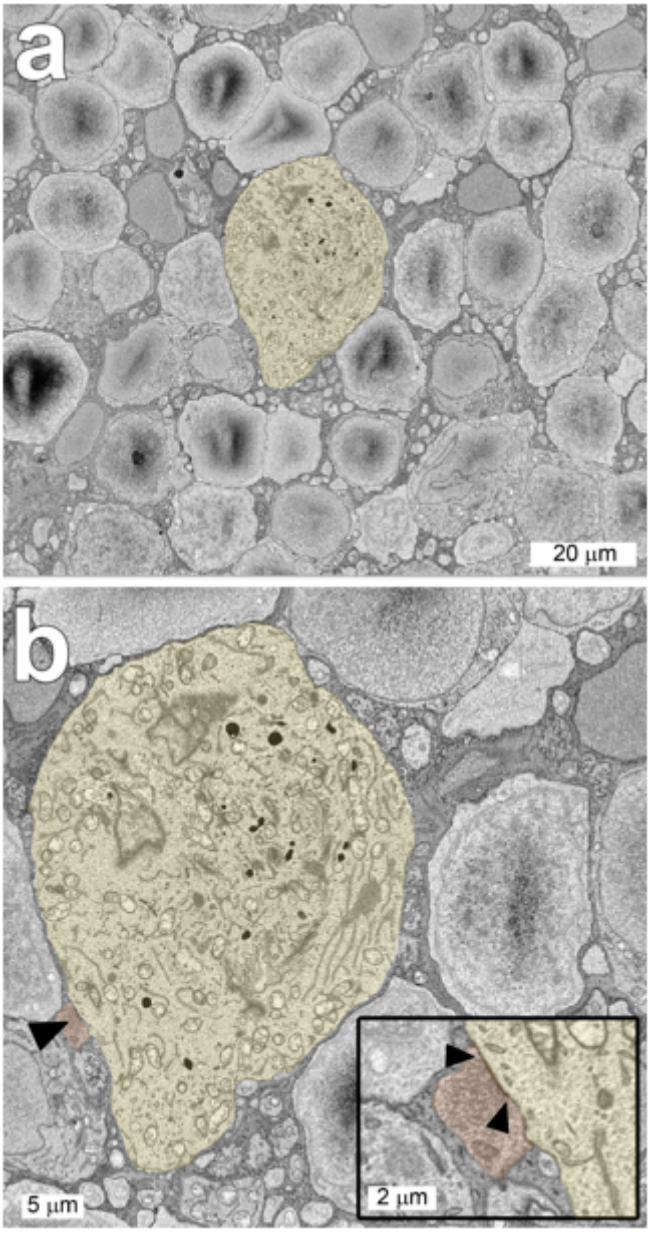

Figure 1

Horizontal sections through the inner nuclear layer of the nasal volume including the soma of gigantic displaced ipRGC 11345. a. Note that the diameter of the ipRGC soma (yellow) was much larger than those of the surrounding cells. b. There was a synapse (▲) from an amacrine cell (orange) onto the primary dendrite of this ipRGC. The boundaries of the synaptic density are indicated at higher magnification in the inset.

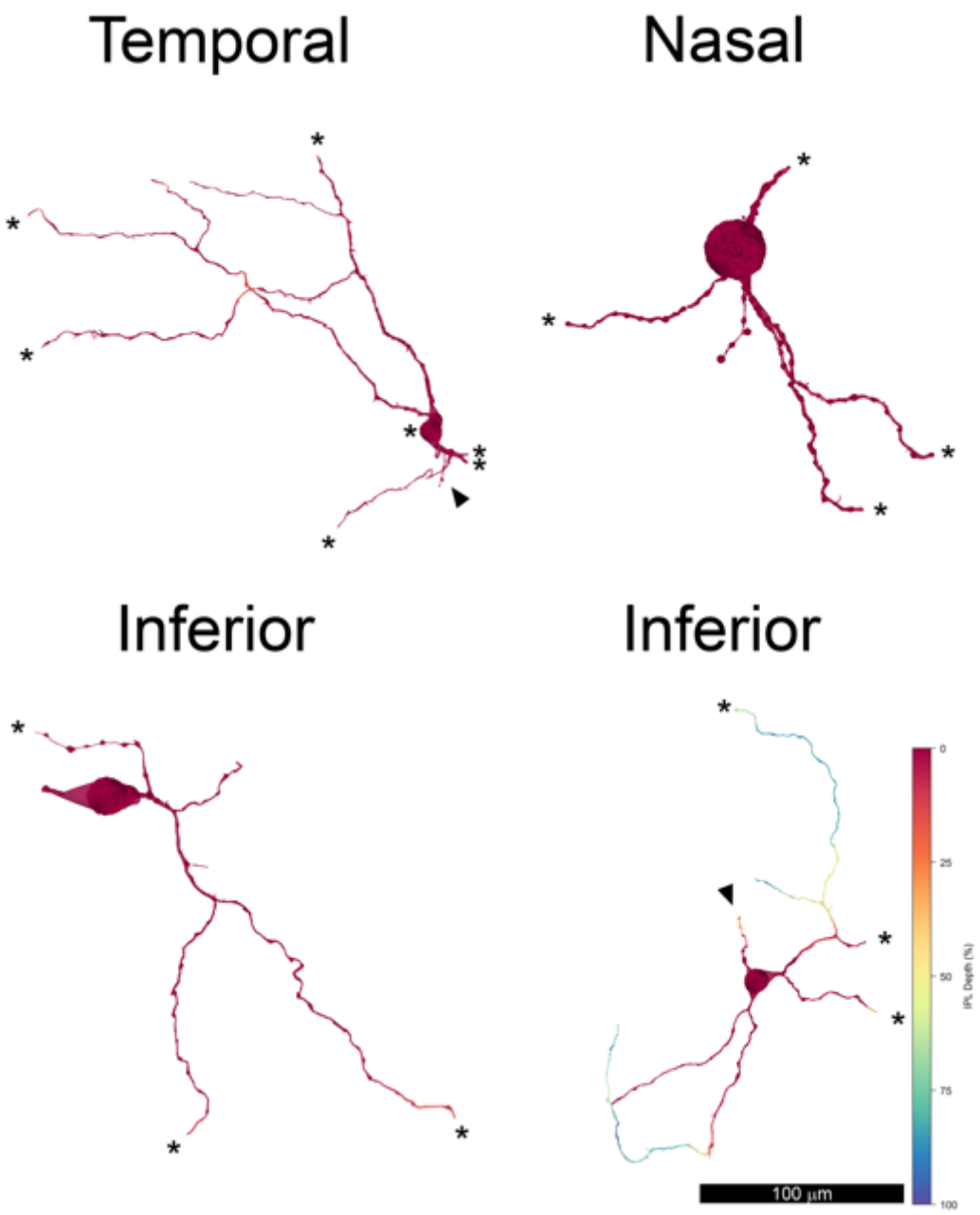

Figure 2

Gigantic displaced M1 ipRGCs were reconstructed in each volume: 6210 temporal, 11345 nasal and 1178 inferior. A smaller, displaced M1 ipRGC, 21551, was also reconstructed in the inferior volume (bottom right). Note that its distal dendrites descended into the inner half of the inner plexiform layer, as indicated

by color in this and in subsequent figures. Some dendrites ran off the edges of the volumes (*), and the axons (▲) were varicose.

Figure 3

Gigantic displaced M1 ipRGC 11345 (yellow) received synapses (▲) from amacrine cells (orange) on its dendrites. Amacrine cells provided the major synaptic input to this and other displaced ipRGCs.

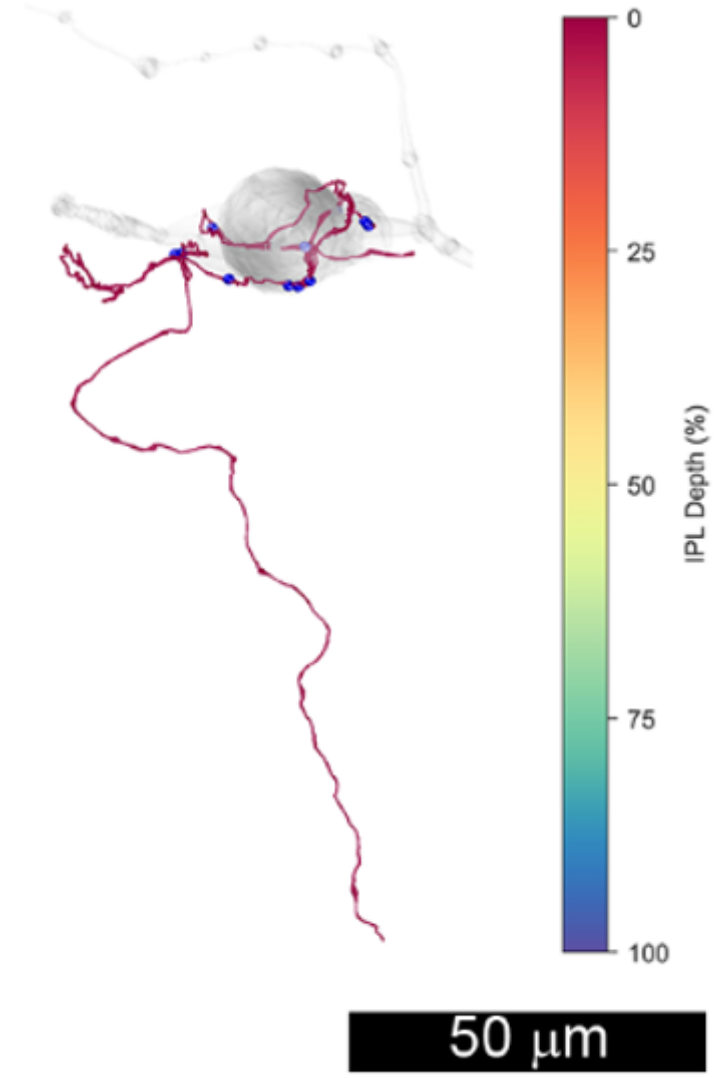

Figure 4

Amacrine cell axon 5560 from the inferior volume was reconstructed. Note that its terminals were found only in the outermost stratum of the inner plexiform layer. It made 11 synapses (●) onto the soma and primary dendrites of ipRGC 1178 (grey). Based on its morphology, it was tentatively identified as an axon of a dopaminergic amacrine cell.

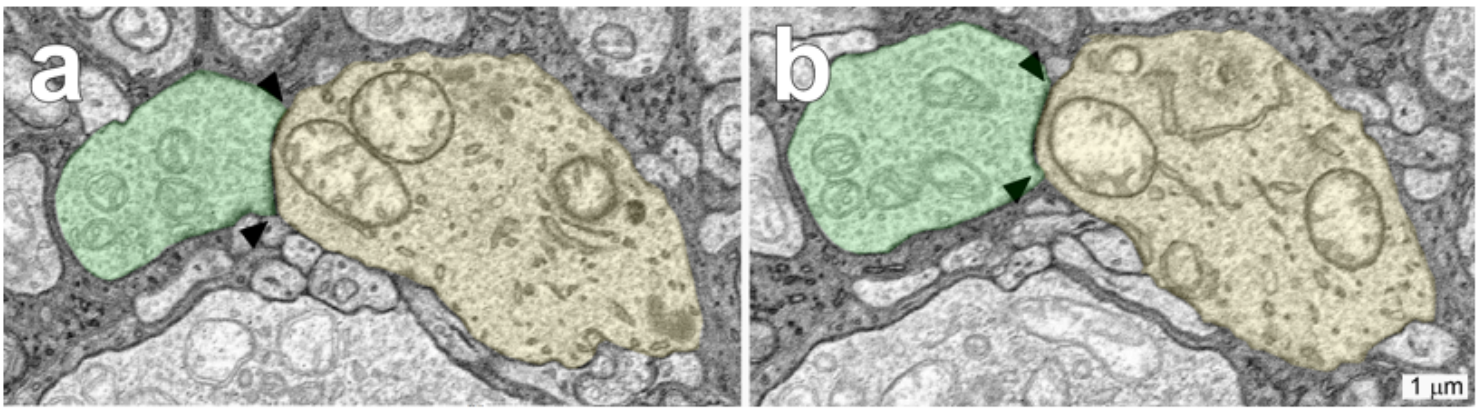

Figure 5

Gigantic displaced M1 ipRGC 11345 in the nasal volume (yellow) received input from a bipolar cell axon (11782, green) at a large non-ribbon synapse (▲). The sections were selected from a series of 18; panel a Z =1885, panel b Z = 1877.

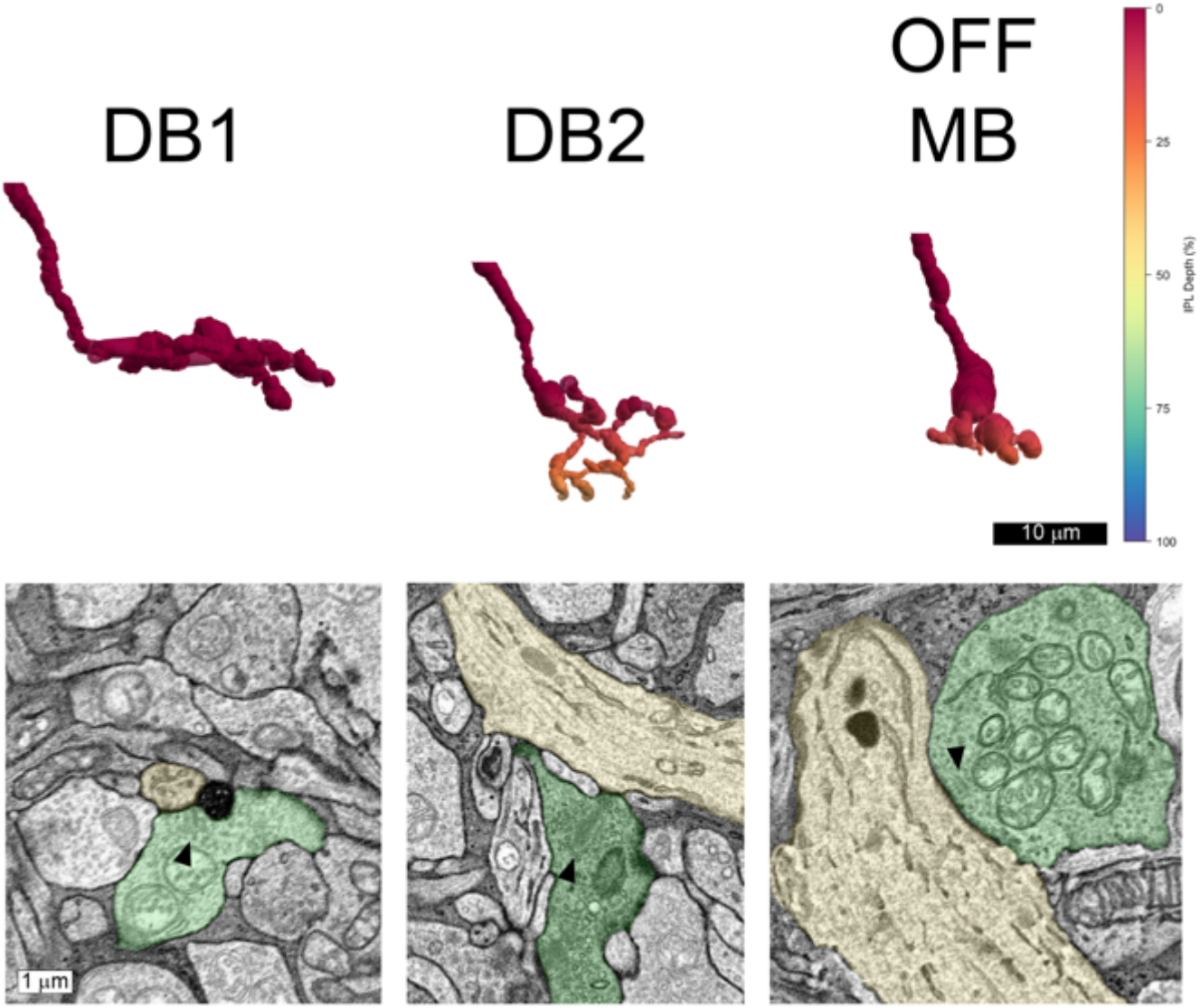

Figure 6

Three types of OFF bipolar cells made synapses onto gigantic M1 ipRGC 11345 in the nasal volume. These include diffuse bipolar (DB) cell 1 (11369), DB2 (14615) and OFF midget bipolar (13313) cells. Their reconstructed axon terminals are shown in the upper panel. Note that none of the telodendria extended into the inner half of the inner plexiform layer. The bipolar cell (green) synapses onto ipRGC 11345 (yellow) are shown in the lower panels, and the synaptic ribbons are indicated (▲).

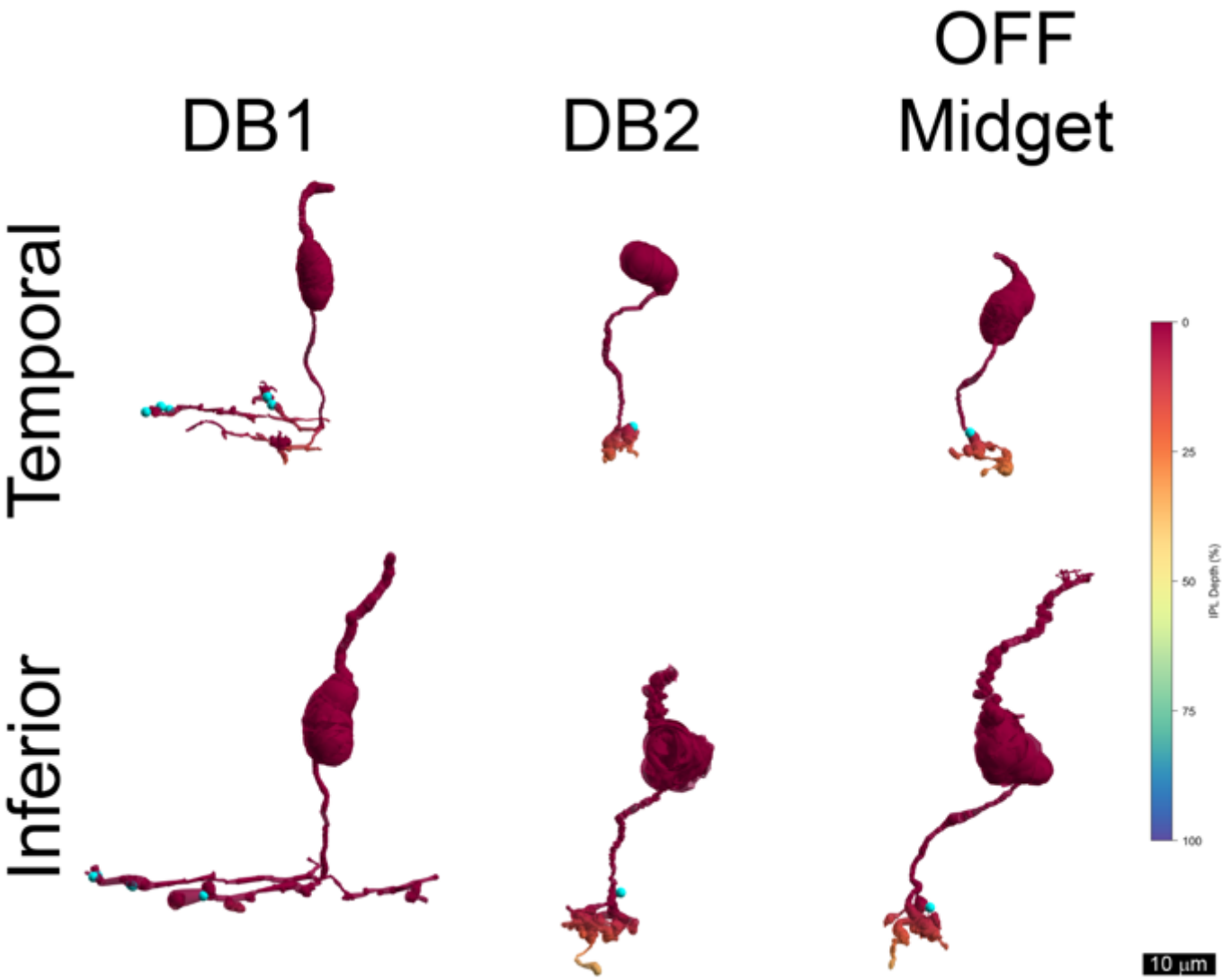

Figure 7

OFF bipolar cell synapses onto gigantic displaced M1 ganglion cells in the temporal (t) and inferior (i) volumes (●). OFF midget = 44052t, DB2 = 44029t, DB1 = 44289t. DB1 = 48234i, DB2 = 48197i, OFF midget = 945i.

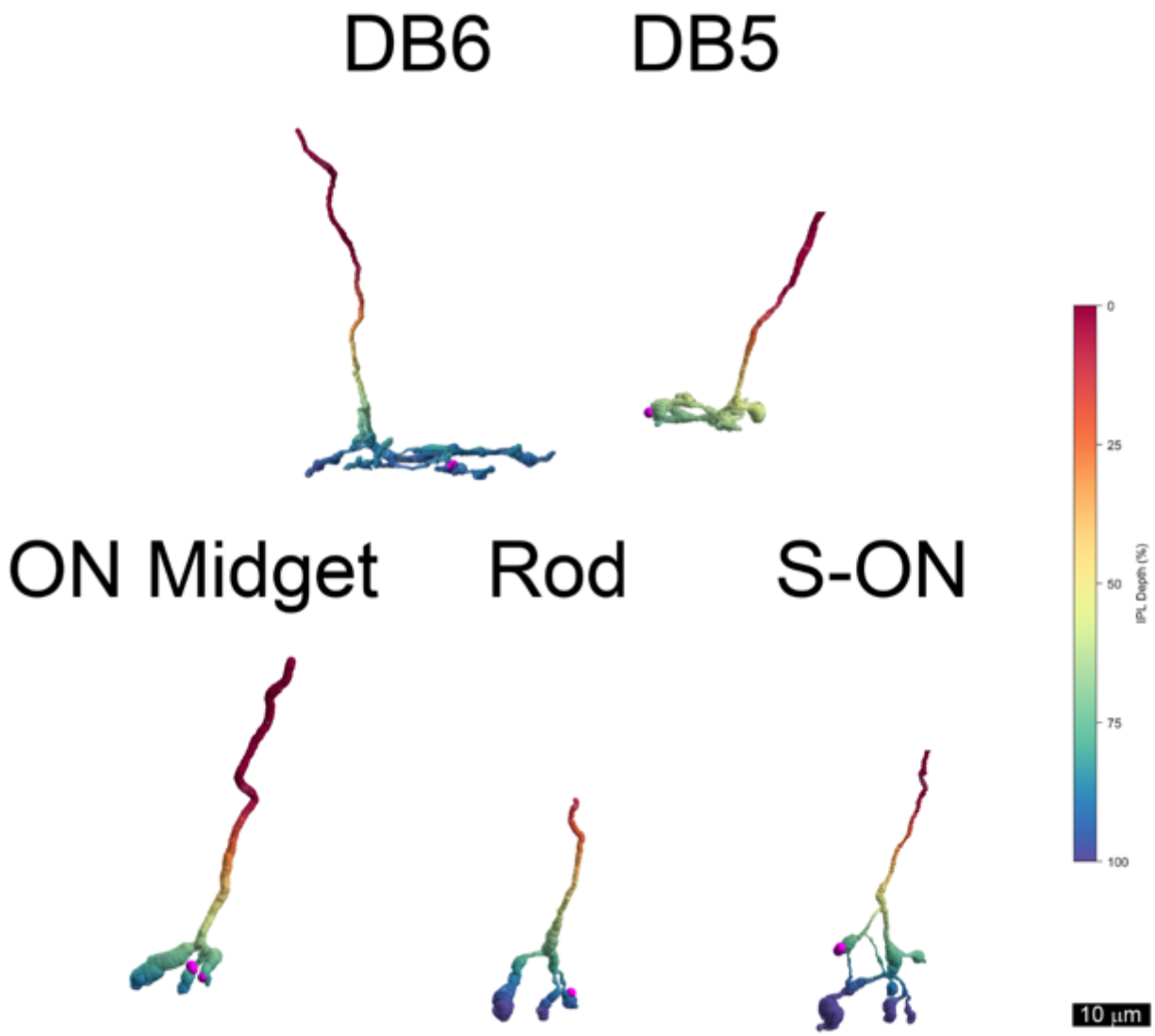

Figure 8

Displaced M1 ganglion cell 2155 received all but one of its excitatory synapses (●) from five types of ON bipolar cells. Note that almost all the bipolar cell synapses are found in the inner half of the inner plexiform layer. DB6 = 43031i, DB5 = 52773i, ON midget = 52770, Rod = 17585i, S-ON = 22103i.